Geomechanics and Engineering, *Vol. 38, No. 6 (2024) 621-631*
https://doi.org/10.12989/gae.2024.38.6.621

Seismic response of operational tunnels to earthquakes with foreshocks or aftershocks

Junyoung Lee[1], Jae-Kwang Ahn*[2] and Byungmin Kim[1]

[1]*Department of Urban and Environmental Engineering, UNIST, 50, UNIST-gil, Eonyang-eup, Ulju-gun, Ulsan, Republic of Korea*
[2]*Earthquake and Volcano Bureau, Korea Meteorological Administration, 61 Yeouidaebang-ro 16-gil, Dongjak-gu, Seoul, Republic of KoreaWuxi, 214122 ,China*

(*Received November 22, 2023, Revised January 23, 2024, Accepted February 24, 2024*)

Abstract. In designing earthquake-resistant structures, we traditionally select dynamic loads based on the recurrence period of earthquakes, using individual seismic records or aligning them with the design spectrum. However, these records often represent isolated waveforms lacking continuity, underscoring the need for a deeper understanding of natural seismic phenomena. The Earth's crustal movement, both before and after a significant earthquake, can trigger a series of both minor and major seismic events. These minor earthquakes, which often occur in short time before or after the major seismic events, prompt a critical reassessment of their potential impact on structural design. In this study, we conducted a detailed tunnel response analysis to assess the impact of both single mainshock and multiple earthquake scenarios (including foreshock-mainshock and mainshock-aftershock sequences). Utilizing numerical analysis, we explored how multiple earthquakes affect tunnel deformation. Our findings reveal that sequential seismic events, even those of moderate magnitude, can exert considerable stress on tunnel lining, resulting in heightened bending stress and permanent displacement. This research highlights a significant insight: current seismic design methodologies, which predominantly focus on the largest seismic intensity, may fail to account for the cumulative impact of smaller, yet frequent, seismic events like foreshocks and aftershocks. Our results demonstrate that dynamic analyses considering only a single mainshock are likely to underestimate the potential damage (i.e., ovaling deformation, failure lining, permanent displacement etc.) when compared to analyses that incorporate multiple earthquake scenarios.

Keywords: earthquake sequences; numerical simulation; permanent displacement; seismic design; tunnel lining

1. Introduction

Tunnels, integral to modern infrastructure, are frequently constructed beneath complex urban landscapes or through challenging mountainous terrains. Such infrastructures offer significant benefits, including reduced travel time and mitigation of the environmental impact by decreased surface land use (McGarry 1968, Zhao *et al.* 2023). However, instances of structural failure can lead to dire situations, such as the entrapment of users. Given the risks, promptly addressing damages, particularly common issues like tunnel lining cracks, is crucial to prevent escalation and more extensive structural damage (Min *et al*. 2021). Therefore, it is important to note that even minor damages in tunnels can significantly disrupt transportation systems and impact vital services (Wang and Zhang 2013).

The seismic waves from earthquakes, as external forces affecting tunnels, are unpredictable and impossible to control, and their impact or risk level is higher than other forces (i.e., geological instability, hydrological changes, construction activity, temperature fluctuations, etc.). Despite this, tunnels have traditionally been perceived as safer than above-ground structures due to their enclosure in soil or rock, which offers some protection against seismic activities (Hashash and Romero-Arduz 2015). However, this perception has changed due to substantial damages observed in several significant earthquakes such as 1999 Chi-Chi earthquake in Taiwan (Wang *et al*. 2001), 2004 Mid-Niigata earthquake in Japan (Jiang *et al.* 2010), and 2008 Wenchuan earthquake in China (Wang *et al.* 2009). These events were marked by extensive ground deformations leading to severe tunnel damages, including collapses in some cases. Additionally, the susceptibility of tunnels to earthquake damage is further highlighted by both severe and minor impacts because minor damage often results in subtle signs, such as water leakage in tunnel linings (Ömer *et al*. 2010). Even these seemingly minor damages can precipitate secondary disasters, emphasizing the need for comprehensive seismic resilience in tunnel maintenance (Kurth *et al.* 2020, Byun and D'Ayala 2022).

Given this context, understanding the seismic design for tunnels becomes crucial. Unlike aboveground structures, tunnels embedded in soil or rock do not experience free vibrations in the same way. This leads to a unique seismic response that is highly dependent on underground movements (Hashash *et al.* 2001, Wang *et al*. 2021). This is the primary reason why the stability of tunnels is influenced by underground movements, especially during seismic events (Aydan *et al.* 2010, Pitilakis and Tsinidis 2013). Experiments have confirmed that the horizontal stress exerted on tunnel linings by seismic waves significantly

*Corresponding author, Ph.D.
E-mail: propjk@korea.kr; propjk@hanyang.ac.kr

ISSN: 2005-307X (Print), 2092-6219 (Online)

exceeds the static stress caused by overburden pressure (Azadi et al., 2020; Wang et al., 2021). Therefore, to assess the stability of tunnel linings against ovaling or racking deformations induced by seismic activity, one can employ analytical solutions (Wang 1993, Penzien 2000). In the analytical solutions, seismic force is evaluated by substituting the maximum shear strain value with a quasi-static load.

The maximum shear strain during an earthquake is determined by the displacement occurring underground. This strain is influenced by the seismic intensity, which in turn is affected by factors such as the earthquake's magnitude, known for peak ground motion acceleration, velocity, and displacement (PGA, PGV, and PGD, respectively) (Schwartz and Coppersmith 1984, Melgar *et al.* 2015). In seismic stability assessments, engineers often rely on seismic intensity values, especially PGA, derived from probabilistic seismic hazard maps based on return periods (Sönmezer and Celiker 2020). However, without specific information about the subterranean medium, direct strain values remain elusive due to the limitations of current prediction methods. Therefore, numerical simulation has been using the analysis of underground structures' behavior (Patil *et al.* 2018; Ahn *et al.* 2018; Sun and Dias 2019, Kang *et al.* 2020).

Additionally, the previously mentioned earthquakes (e.g., 1999 Chi-Chi, 2004 Mid-Niigata, 2008 Wenchuan) had been accompanied by both major seismic events and smaller ones, including foreshock (FS) and aftershock (AS). However, most seismic design methods have not sufficiently considered the phenomenon of earthquake sequences, which become particularly evident during major seismic events. The reason for this is that earthquakes, inherently complex and unpredictable, involve significant uncertainty (Stein *et al.* 2012, Makridakis and Bakas 2016, Xia *et al.* 2017). If codes or standards recommend incorporating earthquake sequences into seismic design and assessments, we can improve our approach to ensuring the safety of infrastructures. Therefore, it is also imperative to give more thought to this phenomenon in seismic design.

Our study adopts an approach distinct from traditional seismic analyses, which often overlook the impact of sequential events such as FSs and ASs. This oversight occurs because, when investigating a collapsed tunnel, we seldom arrive at the scene immediately after an earthquake. Consequently, tunnels that have collapsed due to consecutive earthquakes are sometimes assessed only in the context of major earthquakes. Therefore, our focus is on examining the response of tunnel linings to a series of earthquakes.

2. Earthquake sequence and implications for seismic design

Seismic activity rarely occurs as a standalone event; it typically involves a series of events, including smaller tremors or FSs, a mainshock (the largest event, under MS), and ASs. The occurrence of small earthquakes before and after a major event suggests a complex process of stress

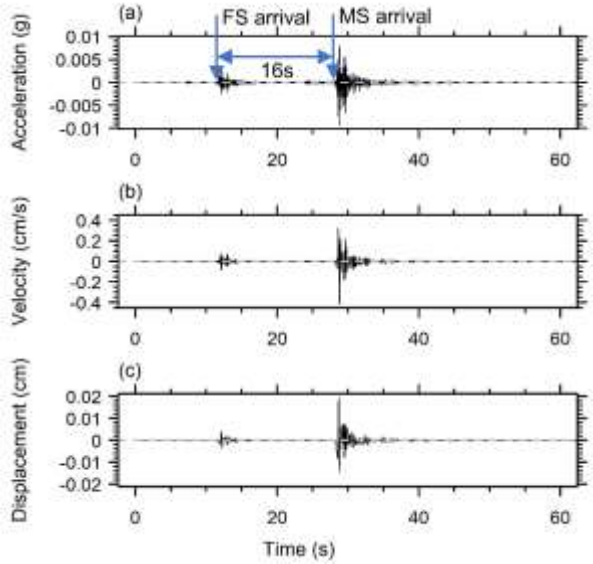

Fig. 1 Goesan sequence earthquake recorded at DGLA stations: (a) acceleration, (b) velocity and (c) displacement

accumulation and release within the Earth's crust (Benioff 1951, Riga and Balocchi 2016). FSs are seen as precursors, indicating the buildup of stress along geological fault lines (Tang *et al*. 2009). Similarly, ASs are part of the process of stress release (Kilb *et al*. 2000).

To understand how these sequences reflect stress processes in the Earth's crust, examining case studies is crucial. For example, the 1999 Chi-Chi earthquake in Taiwan, with a magnitude of 7.6, was followed by 85 ASs of magnitude 5 or greater, demonstrating prolonged stress release (Shin and Teng 2001). The occurrence of a magnitude 6.0 AS within three minutes of the main event highlights the unpredictable nature of seismic sequences.

Similarly, the 2004 Mid-Niigata earthquake in Japan and the 2008 Wenchuan earthquake in China were followed by significant ASs (Shibutani *et al.* 2005, Luo and Liu 2010), emphasizing the need to consider sequences in seismic design due to their ongoing risks.

In the Korean Peninsula, the Pohang and Gyeongju earthquakes is shown that major seismic events are typically accompanied by impactful additional seismic activities (i.e., FS and AS). The Pohang earthquake was followed by a magnitude 4.3 AS two hours after the initial magnitude 5.4 on November 15, 2017, at 03:29:31 UST (Kim *et al.* 2020). The Gyeongju earthquake was preceded by a magnitude 5.1 FS and followed less than an hour later by a magnitude 5.8 MS on September 12, 2016, at 11:32:54 UST (Kim *et al.* 2017). These cases underscore that large earthquakes are typically accompanied by smaller seismic events, which are significant and impactful.

In addition, sometime sequence earthquake both had very short intervals between FS and MS. On October 28, 2022, at 23:27:49 UST, a local magnitude 4.1 earthquake struck 11 km northeast of Goesan-gun, Chungcheongbuk-do (Sheen *et al.* 2023). Here, the critical aspect to note is not the magnitude of the earthquake, but the very short time

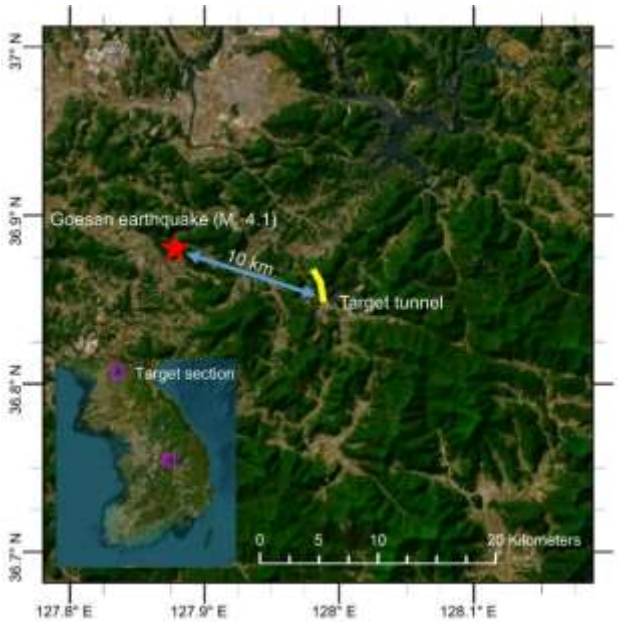

Fig. 2 Locations of Goesan event epicenter and nearby mountain tunnel

Table 1 Ground motions collected

Event name	Station	MS		FS or AS	
		Record date (UTC)	M_L or M_W	Record date (UTC)	M
Gyeongju	EUSB	2016/09/12 11:32:54	5.5	2016/09/12 10:44:32	4.6
Pohang	YOCB	2017/11/15 05:29:31	6.7	2017/11/15 07:49:30	4.8
Goesan	DGLA	2022/10/28 23:27:49	6.5	2022/10/28 23:27:33	6.5
Japan1	GIFH14	2020/04/23 04:44:00	5.5	2020/04/23 04:52:00	4.6
Japan2	IBUH01	2018/09/05 18:08:00	6.7	2018/09/05 18:23:00	4.8
Japan3	ISKH03	2023/05/05 05:42:00	6.5	2023/05/05 05:53:00	5.0
Japan4	KGSH11	2023/08/06 18:12:00	5.4	2023/08/06 18:32:00	4.7
Japan5	MYGH10	2021/02/13 14:08:00	7.3	2021/02/13 14:36:00	4.6
Japan6	MYGH10	2022/03/20 23:44:00	4.3	2022/03/21 00:06:00	4
Japan7	MYZH02	2022/01/21 16:08:00	6.6	2022/01/21 16:21:00	4.5

interval between the FS and the MS, which were only 16 seconds apart. The Goesan earthquake shows similarity to a body wave magnitude 4.5 earthquake that struck Fife, Virginia, U.S., on December 9, 2003 (Kim and Chapman 2005), which also had a 12-second delay between the FS and the MS. Fig. 1 shows the waveforms recorded at the closest stations to the Goesan earthquake sequence. Although these quakes were small in magnitude, the implications of two back-to-back earthquakes are significant. The observed sequences in these case studies suggest that seismic design should not only consider the maximum potential magnitude but also the likelihood and impact of FSs and Ass.

3. Target tunnel and earthquake Scenario

The target tunnel selected for this study is located close to the epicenter of the Goesan earthquake. As illustrated in Fig. 2, this tunnel is situated approximately 10 kms from the epicenter. During the Goesan earthquake, this tunnel did not report any damage, attributed to the earthquake's relatively low magnitude of 4.0. However, this location recalls the case of the Hyogoken-Nanbu earthquake (M_w 6.9, January 17, 1995), which is reported significant damage to tunnels within a 25 kms from the epicenter (Kitagawa and Hiraishi 2004, Roy and Sarkar 2017). If a large magnitude earthquake were to recur in the Goesan area, the target tunnel might experience similar impacts due to its proximity to the epicenter, as observed in Hyogoken-Nanbu event. Hence, this study aims to analyse the potential effects of larger seismic events on tunnels located close to earthquake epicenters.

The ground motions are collected from the stations of Korea Meteorological Administration (KMA). The data recorded from the EUSB station (epicentral distance (R_{epi}): 80.2 km) for a local magnitude (M_L) 5.8 earthquake in Gyeongju on September 12, 2016 and its FS (M_L 5.1), recordings from the YOCB station (R_{epi} = 40.5 km) for a M_L 5.4 earthquake in Pohang on November 15, 2017, and its AS (M_L 4.3), as well as recordings from the DGLA station (R_{epi}= 36.2 km) for a M_L 4.1 earthquake in Goesan on October 29, 2022 and its FS (M_L 3.5). Additionally, we collected 7 pair of MS and AS ground motions from the Kiban-Kyoshin network (KiK-net) database. Table 1 is summarized the information of the origin record in this study.

Given that no structural damage has been reported in the Goesan event, this study aims to create and analyze an earthquake scenario on a scale plausible for the Korean Peninsula. To evaluate the tunnel's response to seismic events arger than those previously recorded in the region, seismograms are adjusted to a target magnitude for input motions from the spectral matching method (SMM). SMM has the advantage of retaining the original record's non-stationary characteristics while matching the target spectrum. Therefore, SMM has been employed to generate the conditions for target scenarios in studies and seismic designs (Hickey and Broderick 2019,Salawdeh 2021,Kwak *et al.* 2022, Yun *et al.* 2024)

SMM is applied for seismic wave correction using SeismoMatch software (SeismoMatch 2020). For the generation of the earthquake scenario larger than record data for tunnel response analyses at the borehole stations, we follow the procedure described below:

Step 1: Select the records nearby seismogram,

Step 2: Calculated spectral acceleration at target location using Ground Motion Model (GMM) for within-motion (Jang *et al.* 2023),

Step 3: Spectrally match the motion from Step 1 to recorded seismogram within from Step 2 using SeismoMatch software.

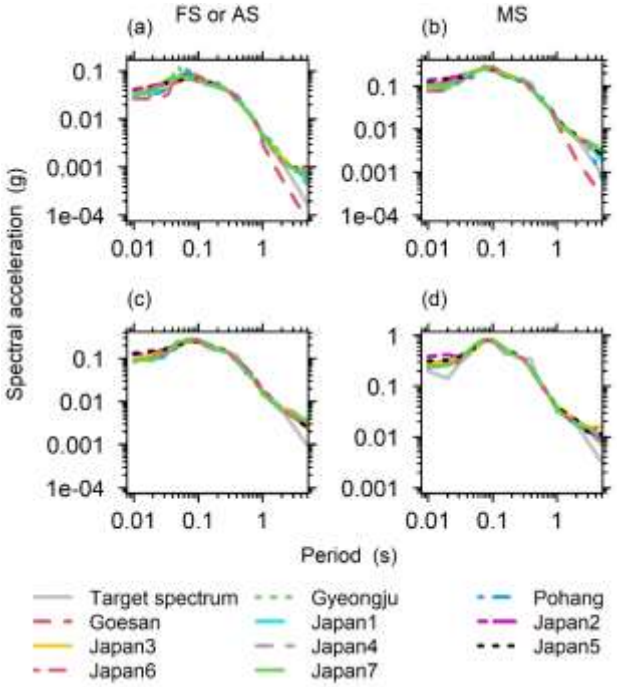

Fig. 3 Matched spectrum accelerations: (a) FS or AS with M_L 5.2, (b) MS with M_L 6.0, (c) FS or AS with M_L 6.0, and (d) MS with M_L 6.0

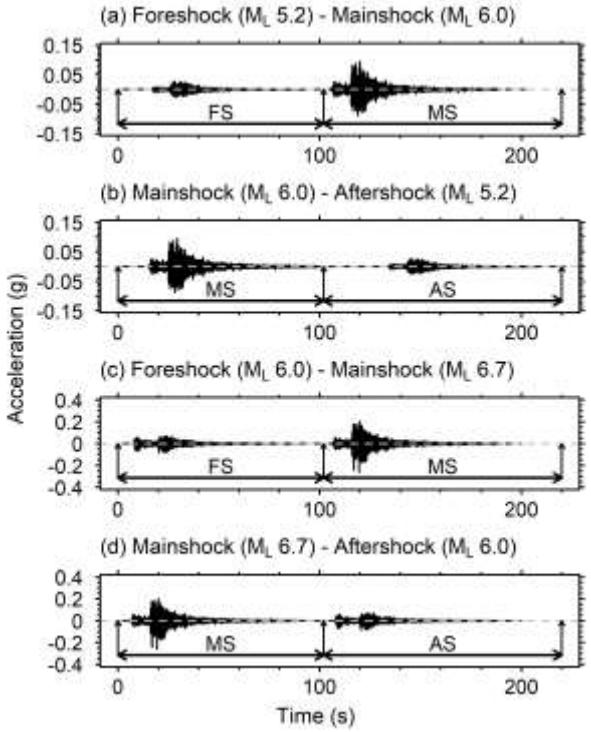

Fig. 4 Combination of matched horizontal seismogram of FS or AS and MS

In Step 3, we employed the matching algorithm (Al Atik and Abrahamson 2010) with 0.3 of tolerance, 50 of max iteration, 0.001 eigen value, and matching period range of 0.02–4 s.

In this process, we matched the collected ground motions to simulate within-motion because the input motion's position is at bedrock, similar to within-rock in numerical simulations. The target spectra are calculated using the within-motion by Jang *et al*. (2023)'s GMM, based on relationships between magnitude and epicentral distance. For this study, we generated record spectra based on earthquakes of magnitudes 5.2, 6.0, and 6.7, considering an epicenter distance of 10 km (Step 2). The generated seismograms are then matched to the selected records (Step 1) according to the results from Step 2. Fig. 3 shows the spectral acceleration of the seismic waves matched for each respective period. We verified the degree of matching level between the spectral acceleration of each adjusted seismogram and the target spectrum, as checked in Fig. 3.

We generated four pairs of scenarios to reflect potential earthquake sequences, such as MS-AS, and FS-MS. As depicted in Fig. 4, we present examples of these scenarios modeled after the Gyeongju event. We combined the matched motions for FS and MS to emulate real earthquake sequences where a MS is succeeded by a FS, or a AS is followed by an MS, all within a brief timeframe of gap under 100 seconds. It's important to note that the gap duration chosen for these simulations is not derived from the actual time intervals between consecutive earthquakes; rather, it's a pragmatic parameter set to streamline the continuity of the analysis.

4. Numerical model and analysis setting

To assess the stability of tunnel deformations induced by earthquake, we could perform analytical solutions (Wang 1993, Penzien 2000) or numerical simulations (Patil *et al*. 2018, Ahn *et al*. 2018, Sun and Dias 2019). In uniformed geology conditions, both methods generally yield similar outcomes (Hashash *et al*. 2005, Ahn *et al.* 2013). However, the application of analytical solutions has limitations since the geo condition in the target location is not uniformed. Therefore, we applied a numerical simulation. A time-domain 2D dynamic numerical analysis is performed based on the excavation tunnel cross-section in mountainous terrain proposed by Ahn *et al*. (2013). A numerical model of the mountainous tunnel is created, as shown in Fig. 5. The ground in the simulation is modelled in such a way that the stress and seismic motion resulting from tunnel excavation did not affect the overall simulation. Additionally, free-field boundaries are introduced at both ends of the model to simulate infinite ground conditions. The uniformed geo-layer 10 meters horizontally on both sides is modelled to apply free-field boundaries. Consequently, aside from the effects at both ends, the model is sufficient to evaluate the impact of mountain tunnels on earthquakes. To consider the both non-linear behavior and large strain, the Mohr-Coulomb model with *Sig 3* (Sigmoidal model) is applied. This law is a non-associative rule, combining hysteretic damping with the elastic-plastic model, specifically the Mohr-Coulomb model. Nonlinear behavior for *Sig 3* is implemented within the elastic range, while plastic deformation occurs when stress-strain exceeded the yield criteria based on the Mohr-Coulomb model. The *Sig 3* model function, employed to simulate the nonlinearity of

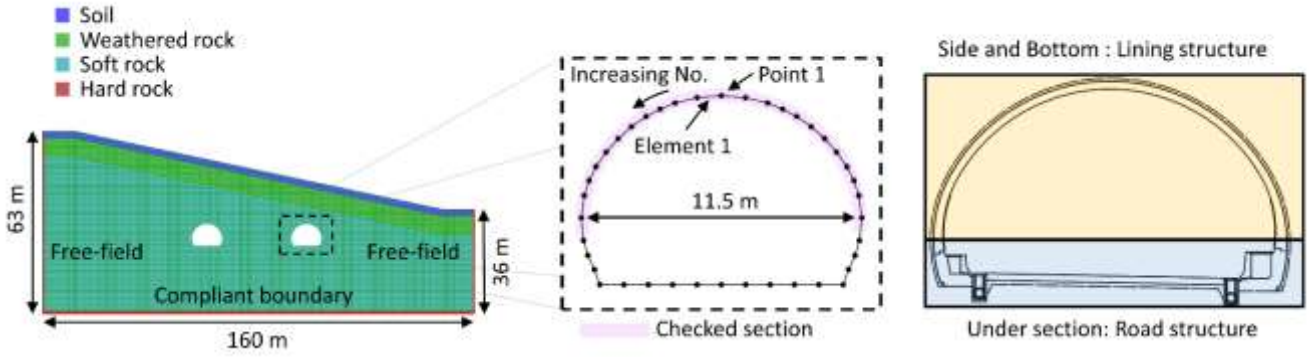

Fig. 5 Modeling of cross-section, boundary condition and tunnel lining

Table 2 Soil Material Properties (Ahn *et al.* 2013)

Soil type	Density (kN/m^3)	Vs (m/s)	Poisson's ratio	Cohesion (kPa)	Friction angle (°)
Soil	18.6	110	0.30	10	27
Weathered rock	21.6	500	0.28	100	30
Soft rock	23.5	1000	0.27	100	30
Hard rock	25.5	1500	0.25	100	30

Table 3 Tunnel Lining Properties (Ahn *et al.* 2013)

Thickness (m)	Elastic Modulus (GPa)	Moment of Inertia (m^4)	Poisson's ratio
0.3	23	0.0025	0.2

Table 4 *Sig 3* fitting variables

Soil type	x_0	a	b	Reference curve
Soil	-1.45	1.0	-0.55	Darendeli (2001)
Weathered rock	-1.70	1.1	-0.56	EPRI (1993)
Soft rock	-1.60	1.1	-0.56	EPRI (1993)
Hard rock	-1.25	1.1	-0.56	EPRI (1993)

the ground, is defined as follows

$$G_{tan}= \frac{a}{1+\exp\left(\frac{x_0-\log(\gamma)}{b}\right)} \quad (1)$$

where G_{tan} represents the tangential shear modulus. x_0, a, and b are curve fitting variables. γ is initial small strain damping at shear strain of 0.0001%.

The properties of the soil and rock are indicated in Table 2. The tunnel lining is modeled as a beam element, and the input material properties are summarized in Table 3. To determine the stresses acting on the lining in the static state, a tunnel excavation analysis with load sharing is performed (Sedarat *et al.* 2009). The information on the target tunnel references from Ahn *et al.* (2013)'s study.

For dynamic analysis, hysteretic damping is employed to consider the nonlinear behavior of the ground. The shear modulus reduction (G/G_{max}) and damping ratio (ζ) curves proposed by Darendeli (2001) for soil and by EPRI (1993) for rock are fitted into *Sig 3* function, which of the coefficients are summarized in Table 4. Free-field boundaries are applied on lateral sides, and a compliant boundary is applied at the bottom to prevent reflection of seismic waves at the as shown in Fig. 5. In the time domain analysis, to consider the damping of the ground at small strain levels where the constitutive model behaves linearly, the Rayleigh damping formula (Rayleigh and Lindsay 1945) is employed. The Rayleigh damping ratio is determined based on the critical damping ratio (ξ_{min}) and center frequency (f_{min}) in the FLAC 2D, and each parameter is calculated as follows (Ahn *et al.* 2013):

$$\xi_{min}= 0.6\,\xi \quad (2)$$

$$f_{min}= 3\,f_{site} \quad (3)$$

where ξ represents the target damping ratio (i.e., 0.03), and f_{site} is the site frequency (i.e., 3.487 Hz in this model).

5. Results

5.1 Assessing of failure section

Initially, the performance of the tunnel lining is assessed based on bending stress. Instead of evaluating axial force (P) and moment (M) demands separately, their interactions are analyzed using a P-M diagram. The threshold for the bending forces of each beam element in the tunnel lining is determined using Response-2000 (Bentz 2000).

Fig. 6 illustrates the P-M interactions of lining elements specifically in one direction tunnel. In Fig. 6, provides a detailed depiction of P-M interactions for the lining with the response of element No. 34 in left tunnel. Black line is criteria of bending failure, which calculated by Response-2000. The blue dot represents the state of the tunnel lining before the earthquake, the red dot shows the P-M at the point where bending stress is maximum during the earthquake, and the black dot illustrates the state after the earthquake.

Prior to the earthquake, the tunnel lining appeared to be in a safe condition. However, during the earthquake, the bending stress momentarily exceeded the allowable value. This element demonstrated a substantial increase in axial force (P) during the seismic events, surpassing the threshold in the P-M correlation diagrams and suggesting potential for

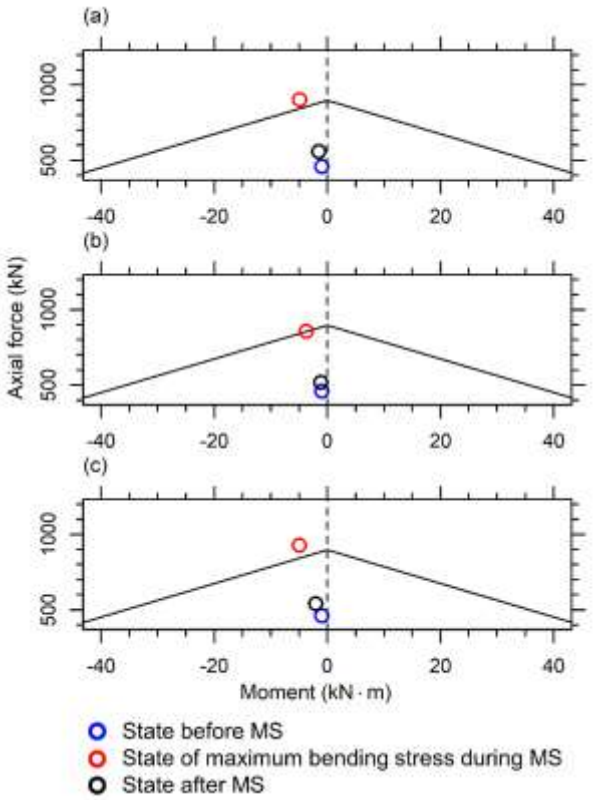

Fig. 6 Response of P-M on No.34 lining elements in left tunnel due to MS with M_L 6.7 (a) Gyeongju, (b) Pohang, and (c) Goesan

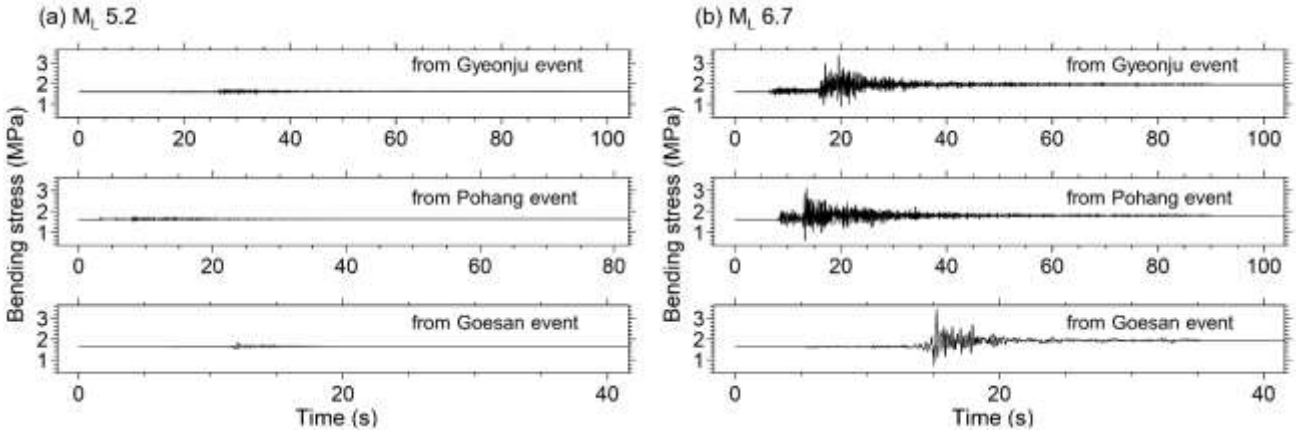

Fig. 8 Bending stress time history at element No.34

concrete destruction. After the shaking ceased, the P-M interactions returned within the criteria for bending failure, yet they did not revert to the initial pre-earthquake state.

This indicates a change in the stress state of the ground before and after the earthquake. In conclusion, M_L 6.7 events reveal that the earthquake exerted significant forces on the tunnel and surrounding ground during the scenarios of three different earthquake events.

The analysis of the tunnel linings using the P-M interaction diagram revealed potential damage sites for two direction tunnels when subjected to a MS with a M_L 6.7. As depicted in Fig. 7, these vulnerable points are situated in the upper-middle section of the tunnel walls, specifically at element number 34 in the left tunnel and element number 36 in the right tunnel. Both elements that experienced failure are located right sides, where the overburden pressure is lower than on the other side. Additionally, the damage showed the ovaling deformation, which is typically induced by horizontal stress during seismic activity.

The bending stress experienced by element 34 in left tunnel is analyzed to determine the impact of varying earthquake sizes and seismograms on bending stress. Figure 8 illustrates how the bending stress changes over time. During the input motion with M_L 5.2, there is a slight change in bending stress compared to its static state. However, the stress appeared to return to a level similar to

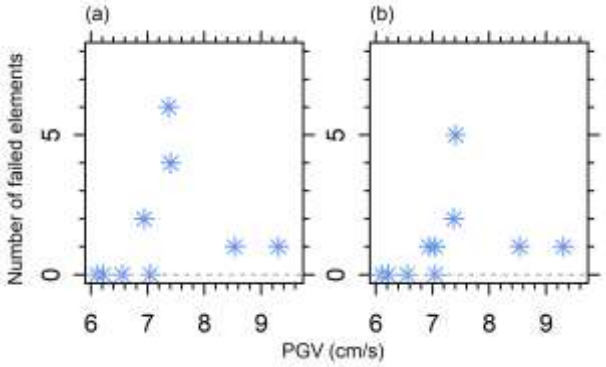

Fig. 9 Number of failed elements on (a) left and (b) right tunnel lining versus PGV

the initial state after the earthquake ended. In contrast, the bending stress during the MS with M_L 6.7 showed a notable difference from the initial state. It is observed that the stress did not revert to its original state once the response acceleration of the targeted section increased. This indicates a potential for long-term damage to the structure.

We calculated number of failed elements on left and right tunnel lining at the maximum bending stress for the scenarios involving M_L 6.0 to 6.7 and compared with the peak ground motion velocity (PGV) as shown in Fig 9. PGV is one of the key parameters in earthquake engineering, is often correlated with the potential for damage to other structures. In this analysis, the PGV is calculated on the input seismograms.

In conclusion, failure occurred in both the left and right tunnels when the PGV exceeded 6.7 m/s. These findings could inform management protocols for tunnel infrastructure, establishing PGV-based standards. We are possible to adapt the Ahn et al. (2023)'s onsite early warning technology, which detects initial P-waves and predicted PGV. Given that the seismic inputs used are derived from records obtained from the KMA's borehole seismometers, it is anticipated that this method will provide adequate early warning for tunnels in the event of an earthquake

5.2 Assessing of permanent displacement

Given that the seismic stability of the tunnel is influenced by relative ground movement, our second investigation focused on assessing permanent displacement (PD). We measure relative displacements of tunnel lining, the displacements of tunnel lining subtracted by the displacements at the free field. Permanent displacements are observed and analyzed, as shown in Fig. 10. Fig. 10 illustrates a time series of the relative displacement at Point 36 on the tunnel lining, providing insights into the effects of the Gyeongju and Japan4 events. The calculated point is located at the upper end of No. 36 element, which influences the lining. We noted that a small amount of PD occurred in the FS, followed by additional PD in the MS. This pattern indicates that sequential seismic events potentially exert a cumulative impact, more substantial than that of a single earthquake.

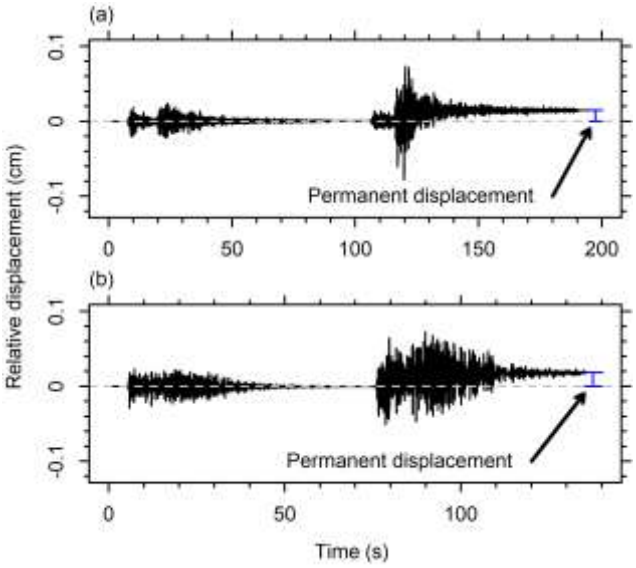

Fig. 10 Relative displacement time series at Point 36 on left tunnel for (a) Gyeongju and (b) Japan4 FS (M_L 6.0) - MS (M_L 6.7)

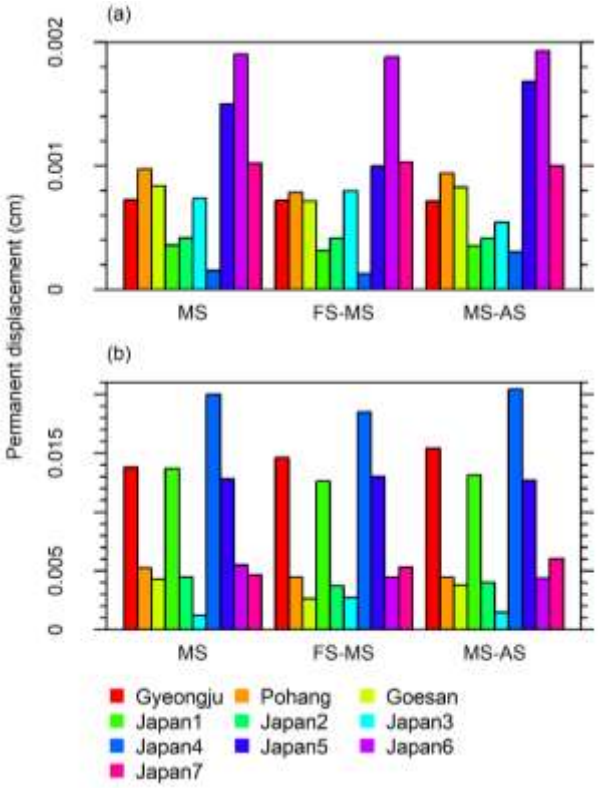

Fig. 11 Permanent displacement at point 36 on left tunnel for (a) MS (M_L 6.0) and AS or FS (M_L 5.2), and (b) MS (M_L 6.7) and AS or FS (M_L 6.0)

Fig. 11 illustrates PDs at point 36 on left tunnel, which are calculated at the ground affected by the lining element for ten pair of input motions for different scenario combinations. In the scenarios involving M_L 5.2 to 6.0, the PDs are less than 0.002 cm (as shown in Fig. 11(a)). This minimal PD is attributed to the limited response displacement of the hard ground (or soft rock) surrounding

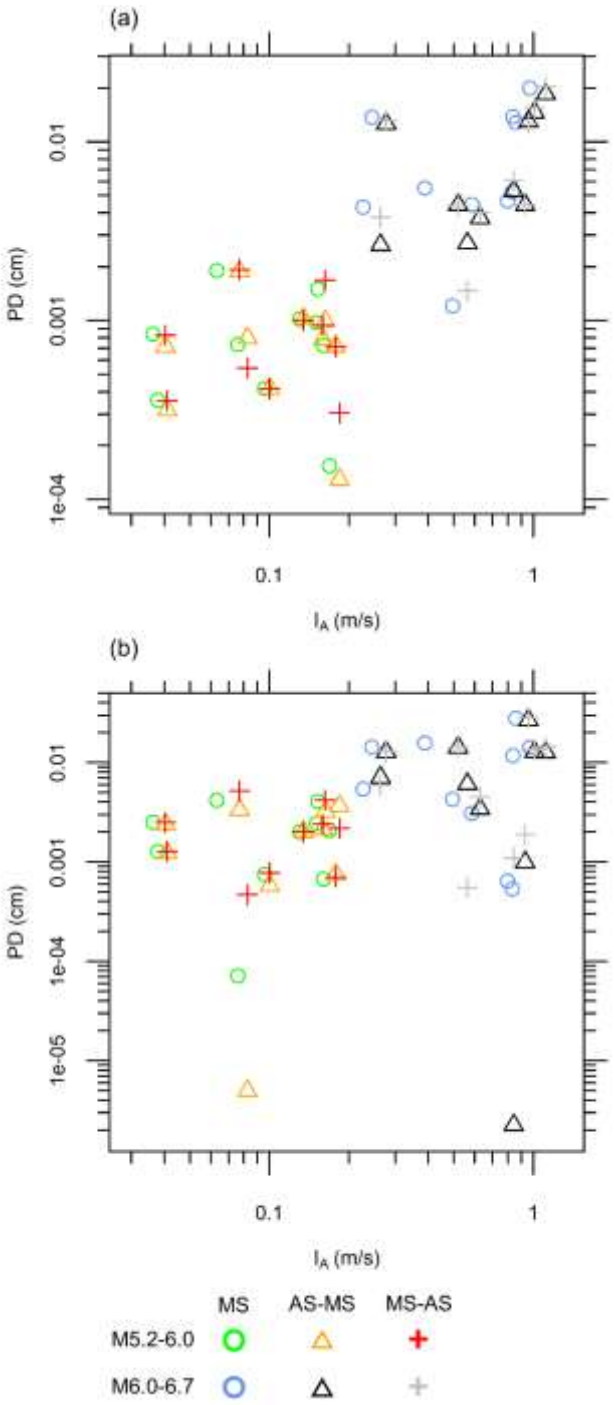

Fig. 12 Permanent displacement on tunnel lining versus arias intensity for (a) Point 36 on left tunnel and (b) Point 36 on right tunnel

the tunnel. Furthermore, it is observed that even if several lower-magnitude earthquakes occur, the overall PD predominantly depends on the MS. Therefore, in low magnitude sequence scenarios, only the main event significantly contributes to the PD.

Fig. 11(b) presents a combination of scenarios on a larger scale than those in Fig. 11(a), specifically involving both of M_L 6.7 to M_L 6.0. Among the three cases calculated, the largest PD occurred in the scenario based on the Japan4 earthquake, with the displacement being about 0.02 cm. Importantly, this finding differs from the previous conclusion that the MS is the primary contributor to overall displacement. In this case, both the FS and AS generated more PD than what is observed when examining the MS alone. This indicates that earthquake sequence may have additional effects on structures.

Fig. 12 illustrates the relationship between Arias Intensity (I_A) and PD for various seismic scenarios. Arias Intensity values are derived directly from the input waveforms used in the analysis. Despite the differences in PD between the left tunnel and the right tunnel locations, a strong correlation is evident between I_A and PD. Notably, the PGA for all input waveforms remained constant, suggesting that when assessing tunnel structures based on earthquake intensity, parameters such as PGV or I_A may offer a more accurate assessment than PGA alone.

Furthermore, the figure highlights the influence of earthquake sequences on PD. It has been observed that the inclusion of foreshocks or aftershocks tends to result in larger PDs compared to scenarios with only a MS. This trend is more pronounced in Fig. 12 compared to Fig. 11, signifying the importance of considering earthquake sequences in seismic analysis. Thus, the data underscore the necessity of incorporating the potential cumulative effects of seismic sequences when evaluating the structural integrity of tunnels.

In additional, we have verified that the combinations caused more PD at scenario based on Gyeongju event. Fig. 13 show the stress-strain curve in the adjacent rock mass to Lining Elements 1 and 34 computed for the dynamic analysis of motions of FS-MS and MS-AS for Gyeongju, respectively. As depicted in Fig. 13b, the upper rock mass adjacent to the tunnel lining displayed an almost linear relationship between stress and strain, indicating no deformation during both the FS and MS phases. However, as illustrated in Figs. 13(c) and 13(d(, both the upper and lower rock masses adjacent to the tunnel sidewall experienced yielding stress during the FS phase, leading to plastic deformation. Additional plastic deformation is observed during the MS phase. This plastic deformation in the rock could potentially influence the permanent displacement of the tunnel lining. In contrast, during the AS phase, the upper and lower rock masses showed only minor additional plastic deformation.

6. Conclusions

In this study, we have carried out a detailed analysis of tunnel behavior under sequential earthquake scenarios. These scenarios were derived from actual earthquake data, with seismograms adjusted to reflect our targeted magnitudes.

Our numerical simulations and analysis focused on tunnel linings. We found that even relatively minor seismic events, if they occur in sequence, can impose significant stress on tunnel structures. This finding suggests that evaluating the impact of main earthquakes alone might underestimate the potential damage, as compared to an

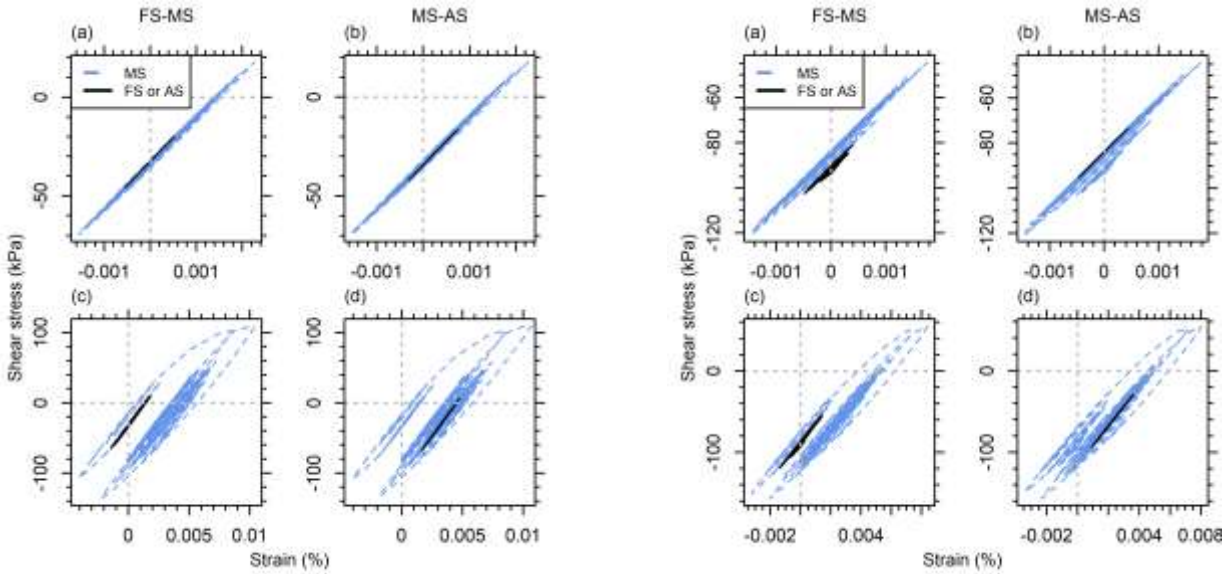

Fig. 13 Stress-strain curves of rocks near element 1 (left) and 34 (right): (a-b) MS of M_L 6 and AS or FS of M_L 5.2, and (c-d) MS of M_L 6.7 and AS or FS of M_L 6 for Gyeongju

assessment that includes the entire sequence of seismic events.

Particularly, our assessment revealed that PD is marginally higher in FS-MS or MS-AS scenarios than in single-event cases. This increase in displacement can be attributed to the ground's response around the tunnel linings. Sequential seismic events can cause additional stress and strain, accumulating damage over time. This is further evidenced by the plastic deformation observed in the upper and lower rock masses adjacent to the tunnel sidewalls during both the foreshock and mainshock phases. Thus, a sequence of earthquakes can result in more significant permanent displacement than a single earthquake event.

In conclusion, our study underscores the importance of considering the cumulative impact of multiple earthquakes, including foreshocks and aftershocks, for a comprehensive assessment of tunnel response and stability. As large earthquakes often involve both FS and MS, overlooking the effects of these sequential events might lead to an incomplete understanding of tunnel behavior. By incorporating the full earthquake sequence into our assessments, we can enhance the safety and durability of tunnel infrastructure in seismically active areas.

While the scenarios examined in our study did not lead to tunnel collapse, our findings show that even earthquakes with the same response spectrum can cause varying degrees of permanent displacement and bending stress, depending on the waveform characteristics. This highlights the need for further research into the diverse impacts of different earthquake scenarios, as examined in our study.

Acknowledgments

The research described in this paper is financially supported by the Natural Science Foundation Korea Meteorological Administration (KMI2021-01910).

References

Ahn, J.K., Park, D.; Kim, D.G. and Kim, K.Y. (2013), "Evaluation of seismic performance of road tunnels in operation", *J. Korean Tunn. Undergr. Sp. Assoc.*, **15**(2), 69-80, (*in Korean*). https://doi.org/10.9711/KTAJ.2013.15.2.069.

Ahn, J.K., Byun Y., Lee, G. and Lee, S. (2018), "A proposal of simple evaluation on the seismic performance of tunnel lining", *J. Korean Tunn. Undergr. Sp. Assoc.*, **20**(2), 361-374, (*in Korean*). https://doi.org/10.9711/KTAJ.2018.20.2.361.

Ahn, J.K., Park, E., Kim, B., Hwang, E.H. and Hong, S. (2023), "Stable operation process of earthquake early warning system based on machine learning: trial test and management perspective", *Front. Earth Sci.*, **11**, 1157742. https://doi.org/10.3389/feart.2023.1157742.

Al Atik, L. and Abrahamson, N. (2010), "An improved method for nonstationary spectral matching", *Earthq. Spectra*, **26**(3), 601-617. https://doi.org/10.1193/1.345915.

Aydan, Ö., Ohta, Y., Geniş, M., Tokashiki, N. and Ohkubo, K. (2010), "Response and stability of underground structures in rock mass during earthquakes", *Rock Mech. Rock Eng.*, **43**(6), 857-875. https://doi.org/10.1007/s00603-010-0105-6.

Azadi, M., Ghasemi, S.H. and Mohammadi, M. (2020), "Reliability analysis of tunnels with consideration of the earthquakes extreme events", *Geomech. Eng.*, **22**(5), 433-439. https://doi.org/10.12989/gae.2020.22.5.433.

Benioff, H. (1951), "Global strain accumulation and release as revealed by great earthquakes", *Geol. Soc. Am. Bull.*, **62**(4), 331-338. https://doi.org/10.1130/0016-7606(1951)62[331:GSAARA]2.0.CO;2.

Bentz, E. (2000), "RESPONSE-2000: load–deformation response of reinforced concrete sections", PhD Dissertation, Department of Civil Engineering, University of Toronto.

Byun, J.E. and D'Ayala, D. (2022), "Urban seismic resilience mapping: a transportation network in Istanbul, Turkey", *Sci. Rep.*, **12**(1), 8188. https://doi.org/10.1038/s41598-022-11991-2.

Darendeli, M.B. (2021), "Development of a new family of normalized modulus reduction and material damping curves", The University of Texas, Austin, Texas, U.S America.

Hickey, J. and Broderick, B. (2019), "Loss impact factors for lifetime seismic loss assessment of steel concentrically braced

frames designed to EC8", *J. Struct. Integr. Maint.*, **4**(3), 110-122. https://doi.org/10.1080/24705314.2019.1622186.
Salawdeh, S. (2021), "Applicability of the direct displacement-based design procedure to concentrically braced frames with setbacks", *J. Struct. Integr. Maint.*, **6**(3), 167-176.
SeismoMatch (2020), "A computer program for adjusting earthquake records to match a specific target response spectrum", Available: http://www.seismosoft.com/seismomatch
Sheen, D.H., Seo, K.J., Kim, S., Kim, B.K., Hong, Y. and Byun, A.H. (2023), "A rapid and automatic procedure for seismic analysis based on deep learning and template matching: A case study on the M 4.1 Goesan earthquake on October 29, 2022", *J. Geol. Soc. Korea.*, **59**(2), 345-354.
Shibutani, T., Iio, Y., Matsumoto, S., Katao, H., Matsushima, T., Ohmi, S., Takeuchi, F., Uehira, K., Nishigami, K., Enescu, B., Hirose, I., Kano, Y., Kohno, Y., Korenaga, M., Mamada, Y., Miyazawa, M., Tatsumi, K., Ueno, T., Wada, H. and Yukutake, Y. (2005), "Aftershock distribution of the 2004 Mid Niigata Prefecture Earthquake derived from a combined analysis of temporary online observations and permanent observations", *Earth Planets Space.*, **57**, 545-549. https://doi.org/10.1186/BF03352590.
Electric Power Research Inst. (1993), Guidelines for determining design basis ground motions. EPRI Research, TR-102293-V5., U.S. America
Hashash, Y.M.A., Hook, J.J., Schmidt, B., John, I. and Yao, C. (2001), "Seismic design and analysis of underground structures", *Tunn. Undergr. Sp. Tech.*, **16**(4), 247-293. https://doi.org/10.1016/S0886-7798(01)00051-7.
Hashash, Y.M.A., Park, D. and Yao, J.I.C. (2005), "Ovaling deformations of circular tunnels under seismic loading, an update on seismic design and analysis of underground structures", *Tunn. Undergr. Sp. Tech.*, **20**(5), 435-441. https://doi.org/10.1016/j.tust.2005.02.004.
Hashash, Y.M.A. and Romero-Arduz, M.I. (2015), Seismic Design of Tunnels, (Eds., M. Beer, *et al*.), Encyclopedia of Earthquake Engineering, 2796-2823. Berlin, Heidelberg: Springer.
Jiang, Y., Wang, C. and Zhao, X. (2010), "Damage assessment of tunnels caused by the 2004 Mid Niigata Prefecture Earthquake using Hayashi's quantification theory type II", *Nat. Hazards*, **53**(3), 425-441. https://doi.org/10.1007/s11069-009-9441-9.
Kang, S.J., Kim, J.T. and Cho, G.C. (2020), "Preliminary study on the ground behavior at shore connection of submerged floating tunnel using numerical analysis", *Geomech. Eng.*, **21**(2), 133-142. https://doi.org/10.12989/gae.2020.21.2.133.
Kilb, D., Gomberg, J. and Bodin, P. (2000), "Triggering of earthquake aftershocks by dynamic stresses", *Nature*, **408**(6812), 570-574. https://doi.org/10.1038/35046046.
Kim, K.H., Seo, W., Han, J., Kwon, J., Kang, S.Y., Ree, J.H., Kim, S. and Liu, K. (2020). "The 2017 ML 5.4 Pohang earthquake sequence, Korea, recorded by a dense seismic network", *Tectonophysics*, **774**, 228306. https://doi.org/10.1016/j.tecto.2019.228306.
Kim, Y., He, X., Ni, S., Lim, H. and Park, S.C. (2017), "Earthquake source mechanism and rupture directivity of the 12 September 2016 M_w 5.5 Gyeongju, South Korea, earthquake", *Bull. Seismol. Soc. Am.*, **107**(5), 2525-2531. https://doi.org/10.1785/0120170004.
Kim, W.Y. and Chapman, M. (2005), "The 9 December 2003 central Virginia earthquake sequence: A compound earthquake in the central Virginia seismic zone", *Bull. Seismol. Soc. Am.*, **95**(6), 2428-2445. https://doi.org/10.1785/0120040207.
Kitagawa, Y. and Hiraishi, H. (2004), "Overview of the 1995 Hyogo-Ken Nanbu earthquake and proposals for earthquake mitigation measures", *J. Japan Assoc. Earthq. Eng.*, **4**(3), 1-29. https://doi.org/10.5610/jaee.4.3_1.
Kurth, M., Kozlowski, W., Ganin, A., Mersky, A., Leung, B., Dykes, J., Kitsak, M. and Kinkov, I. (2020), "Lack of resilience in transportation networks: Economic implications", *Transp. Res. D: Transp. Environ.*, **86**, 102419. https://doi.org/10.1016/j.trd.2020.102419.
Kwak, D., Ahn, J.K., Seo, H., Kang, S. and Kim, B. (2022), "Single-path ground motion amplifications during the 2020 Haenam, South Korea, swarm", *Bull. Earthq. Eng.*, **20**(10), 4937-4959. https://doi.org/10.1007/s10518-022-01386-z.
Lei, X. (2011), "Possible roles of the Zipingpu Reservoir in triggering the 2008 Wenchuan earthquake", *J. Asian Earth Sci.*, **40**(4), 844-854. https://doi.org/10.1016/j.jseaes.2010.05.004.
Luo, G. and Liu, M. (2010), "Stress evolution and fault interactions before and after the 2008 Great Wenchuan earthquake", *Tectonophysics*, **491**, 127-140. https://doi.org/10.1016/j.tecto.2009.12.019.
Makridakis, S. and Bakas, N. (2016), "Forecasting and uncertainty: A survey", *Risk Decis. Anal.*, **6**(1), 37-64.
McAllister, T.P., Wang, N. and Ellingwood, B.R. (2018), "Risk-informed mean recurrence intervals for updated wind maps in ASCE 7-16", *J. Struct. Eng.*, **144**(5), 06018001. https://doi.org/10.1061/(ASCE)ST.1943-541X.0002011.
McGarry, F.J. (1968). "Underground tunnels for transport systems", *Proceedings of the IEEE*, **56**(4), 535-544.
Melgar, D., Crowell, B.W., Geng, J., Allen, R.M., Bock, Y., Riquelme, S., Protti, M. and Ganas, A. (2015), "Earthquake magnitude calculation without saturation from the scaling of peak ground displacement", *Geophys. Res. Lett.*, **42**(13), 5197-5205. https://doi.org/10.1002/2015GL064278.
Min, B., Zhang, C., Zhu, W., Zhang, X. and Li, P. (2021), "Influence of cracks at the invert on the mechanical behavior of the tunnel structures", *Thin-Walled Struct.*, **161**, 107405. https://doi.org/10.1016/j.tws.2020.107405.
Patil, M., Choudhury, D., Ranjith, P.G. and Zhao, J. (2018), "Behavior of shallow tunnel in soft soil under seismic conditions", *Tunn. Undergr. Sp. Tech.*, **82**, 30-38. https://doi.org/10.1016/j.tust.2018.04.040.
Penzien, J. (2000), "Seismically induced racking of tunnel linings", *Earthq. Eng. Struct. D.*, **29**(5), 683-691. https://doi.org/10.1002/(SICI)10969845(200005)29:5<683::AID-EQE932>3.0.CO;2-1.
Pitilakis, K. and Tsinidis, G. (2014), Performance and Seismic Design of Underground Structures, (Eds., M. Maugeri and C. Soccodato), Earthquake Geotechnical Engineering Design, 279-340. Cham: Springer.
Rayleigh, J. and Lindsay, R. (1945), The Theory of Sound. Dover Publications, Inc., Dover.
Riga, G. and Balocchi, P. (2016), "Seismic sequence structure and earthquakes Triggering patterns", *Open J. Earthq. Res.*, **5**(1), 20.
Roy, N., and Sarkar, R. (2017), "A review of seismic damage of mountain tunnels and probable failure mechanisms", *Geotech. Geol. Eng.*, **35**(1), 1-28. https://doi.org/10.1007/s10706-016-0091-x.
Schwartz, D.P. and Coppersmith, K.J. (1984), "Fault behavior and characteristic earthquakes: Examples from the Wasatch and San Andreas Fault Zones", *J. Geophys. Res. Solid Earth*, **89**, 5681-5698. https://doi.org/10.1029/JB089iB07p05681.
Sedarat, H., Kozak, A., Hashash, Y.M.A., Shamsabadi, A. and Krimotat, A. (2009), "Contact interface in seismic analysis of circular tunnels", *Tunn. Undergr. Sp. Tech..*, **24**(4), 482-490. https://doi.org/10.1016/j.tust.2008.11.002.
Shin, T.C. and Teng, T.l. (2001), "An Overview of the 1999 Chi-Chi, Taiwan, Earthquake", *Bull. Seismol. Soc. Am.*, **91**(5), 895-913. https://doi.org/10.1785/0120000738.
Sönmezer, Y.B. and Celiker, M. (2020), "Determination of seismic hazard and soil response of a critical region in Turkey considering far-field and near-field earthquake effect",

Geomech. Eng., **20**(2), 131-146. https://doi.org/10.12989/gae.2020.20.2.131.

Stein, S., Geller, R.J. and Liu, M. (2012), "Why earthquake hazard maps often fail and what to do about it", *Tectonophysics*, **562-563**, 1-25. https://doi.org/10.1016/j.tecto.2012.06.047.

Sun, Q.Q. and Dias, D. (2019), "Assessment of stress relief during excavation on the seismic tunnel response by the pseudo-static method", *Soil Dyn. Earthq. Eng.*, **117**, 384-397. https://doi.org/10.1016/j.soildyn.2018.09.019.

Tajima, R. and Tajima, F. (2007), "Seismic scaling relations and aftershock activity from the sequences of the 2004 mid Niigata and the 2005 west off Fukuoka earthquakes (Mw 6.6) in Japan", *J. Geophys. Res. Solid Earth*, **112**(10). https://doi.org/10.1029/2007JB004941.

Tang, C., Ma, T. and Ding, X. (2009), "On stress-forecasting strategy of earthquakes from stress buildup, stress shadow and stress transfer (SSS) based on numerical approach", *Earthq. Sci.*, **22**, 53-62. https://doi.org/10.1007/s11589-009-0053-y.

Wang, C., Ding, X., Chen, Z., Feng, L. and Han, L. (2021), "Seismic response of utility tunnels subjected to different earthquake excitations", *Geomech. Eng.*, **24**(1), 67-79. https://doi.org/10.12989/gae.2021.24.1.067.

Wang, J.N. (1993), Seismic design of tunnels: A state of the art approach. (Vol. Monograph 7). Parsons Brinckerhoff Inc., One Penn Plaza, New York., U.S. America.

Wang, T.T., Kwok, O.L.A. and Jeng, F.S. (2021), "Seismic response of tunnels revealed in two decades following the 1999 Chi-Chi earthquake (Mw 7.6) in Taiwan: A review", *Eng. Geol.*, **287**, 106090.

Wang, W.L., Wang, T.T., Su, J.J., Lin, C.H., Seng, C.R. and Huang, T.H. (2001), "Assessment of damage in mountain tunnels due to the Taiwan Chi-Chi Earthquake", *Tunn. Undergr. Sp. Technol.*, **16**(3), 133-150. https://doi.org/10.1016/S0886-7798(01)00047-5.

Wang, Z., Gao, B., Jiang, Y. and Yuan, S. (2009), "Investigation and assessment on mountain tunnels and geotechnical damage after the Wenchuan earthquake", *Sci. China Technol. Sci.*, **52**(2), 546-558. https://doi.org/10.1007/s11431-009-0054-z.

Wang, Z.Z. and Zhang, Z. (2013), "Seismic damage classification and risk assessment of mountain tunnels with a validation for the 2008 Wenchuan earthquake", *Soil Dyn. Earthq. Eng.*, **45**, 45-55. https://doi.org/10.1016/j.soildyn.2012.11.002.

Xia, Y., Xiong, Z., Dong, X. and Lu, H. (2017), "Risk assessment and decision-making under uncertainty in tunnel and underground engineering", *Entropy*, **19**(10), 549. https://doi.org/10.3390/e19100549.

Yun, J.W., Han, J.T. and Ahn, J.K. (2024), "Acceleration amplification characteristics of embankment reinforced with rubble mound", *Geomech. Eng.*, **36**(2), 157-166. https://doi.org/10.12989/gae.2024.36.2.157.

Zhao, D., Tu, H., He, Q. and Li, H. (2023), "Research on the design and construction of inclined shafts for long mountain tunnels: A review", *Sustainability*, **15**(13). 9963. https://doi.org/10.3390/su15139963.